

Micro-Raman analysis of glisterings in intraocular lenses

G. Rusciano^{a,b}, A. Martinez^a, G. Pesce^a, G. Zito^a and A. Sasso^{a,b}

^aDepartment of Physics "E. Pancini", University of Naples Federico II
Compl. Univ. M.S. Angelo, via Cinthia
80126, Naples - Italy

^bNational Institute of Optics (INO-CNR), c/o Comprensorio Olivetti Via Campi
Flegrei 34 - 80078 Pozzuoli (NA)

ABSTRACT

The phenomenon of inclusions or microvacuoles in intraocular lenses (IOL), often referred to glistenings due to their appearance when visualized in slit-lamp exams, is main cause of decreased visual in people after IOL implantation. For this reason, there is a huge request by the market of new polymers able to reduce, or even eliminate, the formation of such microvacuoles. In such frame, the use of advanced optical techniques, able to provide a deeper insight on the glistening formation, is strongly required. In particular, Raman spectroscopy (RS) is ideally suited for the analysis of polymers, due to its well-know sensitivity to highly polarizable chemical groups, commonly found in the polymer chains backbones. Moreover, the combination of RS with optical microscopy (Raman micro-spectroscopy) paves the way for real, information-rich chemical mapping of polymeric materials (Raman imaging). In this paper, we analyze the formation of microvacuoles in IOLs following a thermal treatment. In particular, we performed a chemical mapping of a single microvacuole, which allowed us to infer on its effective chemical composition. In order to investigate on the reversibility of glistenings formation, this analysis was repeated as function of time after thermal treatment, in different IOL environments. It turns out that this phenomenon is partially reversible, with an almost complete disappearance of microvacuoles in a dry environment.

Keywords: Intra Ocular lenses, IOLs, Glistenings, Raman spectroscopy

1. INTRODUCTION

Intraocular lenses (IOLs) are well-established medical devices routinely used to replace the natural crystalline lens when it is affected by cataract or other degenerative processes, which alter the normal transparency of the natural lens [1].

The materials used for IOLs have been evolving since the first modern demonstration in 1949 in which PMMA (polymethylmethacrylate) successfully replaced the first attempts based on glass materials [2]. Later, at the beginnings of 1980s, the advent of flexible materials like silicone allowed to implant soft IOLs through narrower incisions [3], thereby reducing patient recovery time. The rise of foldable lenses have led to the development of a wide spread versions of flexible IOLs on the market (PMA, PEMA, HEMA etc.) [4, 5].

Nowadays IOL implantation is one of the most common surgical procedures performed in the world with almost 20 millions per year, a level that will surely increase in view of the more recent use of IOLs for treatment of myopia and hyperopia. Within this scenario new polymer materials have been introduced to satisfy high levels of biocompatibility, flexibility and optical functions.

Considering the huge number of implanted IOLs even a small percentage of negative optical conditions may have significant negative impact on the patients. The phenomenon of glistenings is one of the most disturbing effect that

occurs in patients who wear IOLs for a number of years after implantation. At the slit lamp examination, it appears as “glistening” within the IOLs caused by the scattering from inclusions not observable at the time of implantation [6]. When the size and the number of these defects exceed a certain threshold the vision quality of the patient can be compromised [7]. The phenomenon of glistenings was first observed in hydrophobic acrylic IOLs but it was also verified in different IOL materials, including silicone, hydrogel and poly(methyl methacrylate). The available literature describes the occurrence time of glistening to vary from few weeks up to several months postoperatively [8]. Glistenings are usually distributed throughout the entire IOL optic. Typical size of microvacuoles ranges from few μm to 10 μm clinically observed. Larger sizes (up to 20 μm) may be observed during in vitro studies induced by submitting the IOLs to thermal shock in water. Typically, glistening tends to disappear when IOLs are removed from water and dried. Multiple studies have evaluated the possible mechanism of glistening formation within IOLs [for a review see ref.[8]]. There are two main theories proposed for the formation of glistening. The first one suggests that polymers absorb water when immersed in an aqueous environment over an extended period of time. If the absorbed water fills a void within the polymer network of the IOL, a visible water drop forms. The difference between the refractive index of water and that of polymer gives place to the scattering of the formed microvacuoles. According to a more recent theory cavity development are attributed to osmotic pressure differences between the cavity and the liquid in which IOL is embedded. The glistenings are the result of hydrophilic impurities within the IOL material either initially present as second phase particles or ascribable to hydrolysis caused by aging. In this paper we propose to investigate the biochemistry nature of microvacuoles by using Raman spectroscopy to shed light on the still not yet clarified mechanisms at the basis of glistenings. Raman spectroscopy, combined with confocal optical microscopy, is an ideal tool for this kind of investigation, offering high spatial resolution and high chemical selectivity due to the fingerprinting character of the Raman spectra.

2. RESULTS AND DISCUSSION

2.1 Optical Measurements

The materials of IOLs here examined are typical of acrylate copolymers commonly found in commercial IOLs. We considered two types of materials, hereinafter denote IOL *A* and *B*. IOL *A* exhibited a conventional opacity while in IOL *B* the phenomenon was almost negligible. In the latter case, the polymer blend was modified in order to reduce the internal hydrophobicity of the material without increasing the hydration of the polymer coefficient (which remains around 1%). In such way, we observed that the formation of micro bubbles keeping IOL lenses in an aqueous solution at a temperature of 36 °C, was almost prevented. Both materials examined have a glass transition temperature below the physiological temperature and refractive index around 1.5. Main physical parameters of used IOLs are listed in Table I.

Table 1. Physical parameters of the IOLs used in this experiment.

POLYMER	REFRACTIVE INDEX	GLASS TRANSITION TEMPERATURE	WATER ABSORPTION	OPTICAL POWER
IOL - TYPE A	1.526(#546 nm)	12°C	1.1 %	20 D
IOL - TYPE B	1.506(#546 nm)	8°C	2.9 %	20 D

IOLs were first observed with an optical microscope, observing regions of the IOL at different position in the transverse x-y plane and at different axial penetration z inside the IOL. Figure 2, part (A) shows typical optical images obtained just after the induction of glistenings for both IOL A and IOL B. nm

As expected, for IOL A the inner part of the material is crowded by many microvacuoles whose size ranges from 5 to 15 μm . The number of bubbles decreased considerably after one day from glistenings. On the contrary IOL B exhibited a much lower number of microvacuoles and, not rarely, whole field of view of the microscopes appeared completely empty of micro vacuoles.

The degree of opacity of our IOLs was measured by means of a spectrophotometer (PerkinElmer Lambda 35 UV/VIS) by recording the transmittance curves after that IOLs were kept for 5 h at a temperature of 48 °C. In Fig. 1, part (B) is compared the time evolution of the transmittance at different time after the thermal shock both for IOL A and B. As it can be noted the IOL A, at t=0, exhibits a transmittance of ~45%. Afterwards the transmittance start to recover, and it reaches a steady state transmission around 95% after ~24 h. Differently, for IOL B, just after glistenings, the transmittance is slightly reduced to 90-95 %, and a full recovery occurs with the same time.

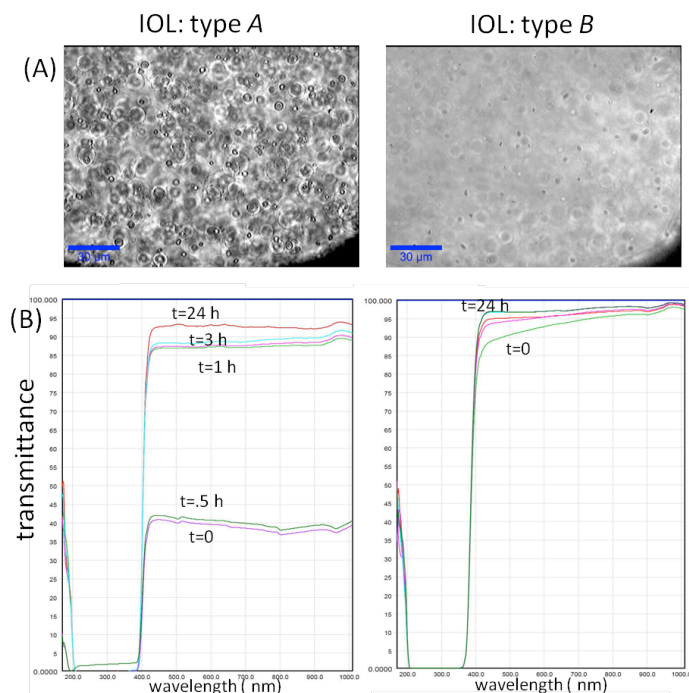


Figure 1. (A) Typical optical images of IOL: type A, left, and type B, right. Images correspond to a depth of 100 μm inside the IOL. (B) Transmittance curves at different times after the induction of glistenings (t=0, 0.5, 1, 3, and 24 hours) for both IOLs A and B.

2.2 Raman Measurements

Raman measurements were performed with a commercial system (*Witec Alpha 300*) based on a laser source emitting at 532 nm ($P_{\max}=25$ mW). For details see ref. [9,10]. We first record the Raman spectra in a point of the IOL free of microvacuoles before and after glistenings to check that the thermal shock does not induced any change in the chemical structure of the polymer. Then we scanned the laser in a region of the IOL $30\ \mu\text{m} \times 30\ \mu\text{m}$ wide (scan step = $1\ \mu\text{m}$, laser power = 25 mW, acquisition time = 1s for single spectrum) to explore the heterogeneity of the sample. We noted a maximum excursion of about 10% by monitoring the intensity of the band between 2800 and $3000\ \text{cm}^{-1}$, ascribable to CH stretching modes.

Afterward, we focused on a single isolated microvacuole (see Fig. 2 A) performing a raster scan around it in a region slightly wider than the size of the microvacuole itself (scan width = $16\ \mu\text{m} \times 16\ \mu\text{m}$). Typical spectra observed inside and outside the microvacuole is reported in Fig. 3B. What can be observed is that the spectrum obtained internally to the bubble is similar to that externally, except the band between 3300 and $3650\ \text{cm}^{-1}$, corresponding to the O-H stretching mode of water. Interestingly, unlike common interpretation reported in literature, this demonstrates that the so called microvacuoles are not empty cavity filled by water but, in some manner, water lies in a complex network. This result can be explained in view of the complex dynamic of polymerization. As a matter of facts, the bulk polymer net is not completely connected, and the polymer chains are not perfectly folded. As a consequence, regions with lower density can appear, which can be prone to be filled with water. This also explains the observed Raman intensity fluctuations of $\sim 10\%$ before the induction of glistenings. Moreover, it should be observed that copolymer blends present many cross-linked chains which involve hydrophilic and hydrophobic part of the single polymer constituents. This reasonably gives place to the formation of cages which behaves as a sponge for the water. A Raman image of a single microvacuole in terms of the polymer contribution (band between 2800 and $3000\ \text{cm}^{-1}$) and water (band between 3300 and $3650\ \text{cm}^{-1}$) is shown in Fig. 2 (B) and (C), respectively. From preliminary measurements of pure polymer and pure water samples we can infer a relative concentration water/polymer of the order of 5%.

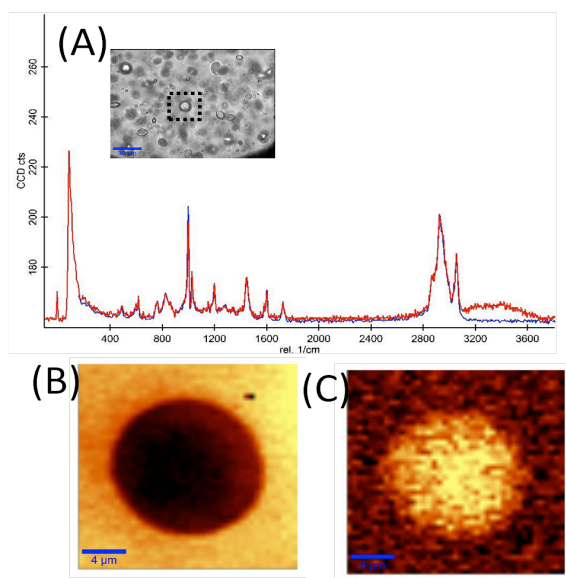


Figure 2. (A) Typical Raman spectra recorded in a point external (blue curve) and internal (red curve) to the selected microvacuole (see the inset which shows the optical image of the analysed microvacuole). (B) Raman imaging around the selected microvacuole shown in the inset of part (A), obtained by plotting the intensity of the polymer band between 2800 and $3000\ \text{cm}^{-1}$ (B) and that of the water band between 3300 and $3650\ \text{cm}^{-1}$.

As final step, we investigated the evolution of a single microvacuole in dry environment. Fig. 3 reports the Raman imaging at different times (indicated in the single panels) after the IOL exposure to air, as well as a wide-field optical image obtained at $t=0$, in which IOL was removed from the liquid environment in which glistening was induced by the thermal treatment indicated above. In particular, the Raman maps correspond to the intensity of the features in the 2800 - $3000\ \text{cm}^{-1}$. Clearly, there is a marked decrease of microvacuole, which tend to disappear after 24 h.

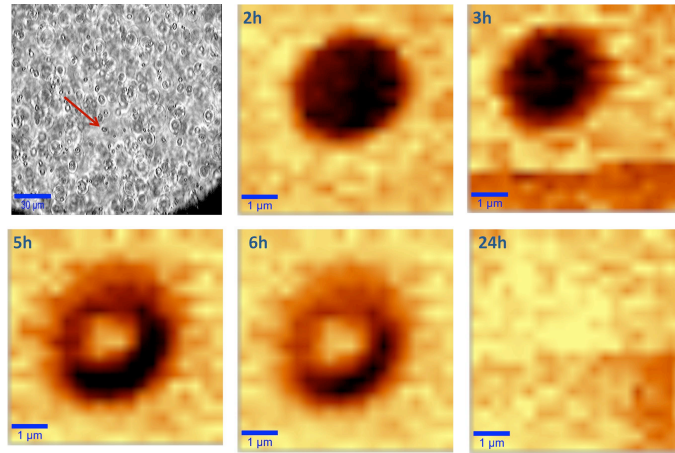


Figure 3. Wide field optical image (top-left panel) and Raman maps of a single microvacuole obtained after IOL exposure to air. Labels in the single panel indicated the time elapsed from the IOL removal from the liquid environment. The red arrow in the top-left panel indicates the microvacuole undergoing to Raman analysis.

3. CONCLUSIONS

In this work we have demonstrated the possibility of using Raman micro-spectroscopy for the study of glistenings in intra ocular lenses. In particular, we have investigated the biochemical composition of a single microvacuole finding that it is composed of a mixing of the polymer matrix and water. This study, therefore, opens the way for a systematic analysis of the appearing and recovery of glistening at a micrometric scale in various materials used for IOLs fabrication undergone to different experimental conditions (physiological saline solutions, thermal cycles, etc.).

4. REFERENCES

- [1] Leaming, D., "Practice styles and preferences of ASCRS members," *J. Cataract Refract. Surg.* 21:378–385 (1995).
- [2] Ridley H., "Intra-ocular acrylic lenses: a recent development in the surgery of cataract" *Br. J. Ophthalmol.* 36, 113–122 (1952).
- [3] Epstein E., "Use of soft lenses" *J. Cataract Refract. Surg.* 16:779- (1990).
- [4] Manfred T., and Matthew R. J. "New hydrophobic IOL materials and understanding the science of glistening" *Current Eye Research*, 40, 969–981 (2010).
- [5] Tripti D., Haldar R.S., Geetha S., Niyogi K., Khandal R.K. "Materials for intraocular lenses (IOLs): Review of developments to achieve biocompatibility e-Polymers 124, 1-23 (2009).
- [6] Dhaliwal, D., Mamalis, N., Olson, R., Crandall, A., Zimmerman, P., Aldrege, O., et al. "Visual significance of glistenings seen in the acrysof intraocular lens" *J. Cataract Refract. Surg.* 22, 452–471 (1996).
- [7] Gunenc., U, Oner., F, Tongal, S., Ferliel, M. "Effects on visual function of glistening and folding marks in acrysof intraocular lenses" *J. Cataract Refract. Surg.* 27, 1611–1614 (2001).
- [8] Werner, L. "Glistenings and surface light scattering in intraocular lenses" *J. Cataract Refract. Surg.* 36, 1398–1420 (2010).
- [9] Rusciano, G., Capriglione, P., Pesce, G. Del Prete, S., Cennamo, G., Di Cave, D., Cerulli, L., Sasso, A., "Raman microspectroscopy analysis in the treatment of *acanthamoeba* keratitis", *PLOS ONE* 8, e72127 (2013).
- [10] Rusciano, G., Zito, G., Pesce, G., Del Prete, S., Cennamo, G., Sasso, A., "Assessment of conjunctival microvilli abnormality by micro-Raman analysis" *J. Biophotonics* 9, 551-559 (2016).